

Entanglement dynamics under decoherence: from qubits to qudits

A.R.R. Carvalho^{1,2,a}, F. Mintert^{1,3}, S. Palzer¹, and A. Buchleitner¹

¹ Max-Planck-Institut für Physik komplexer Systeme, Nöthnitzer Strasse 38, 01187 Dresden, Germany

² Department of Physics, Faculty of Science, The Australian National University, ACT 0200, Australia

³ Department of Physics, Harvard University, Cambridge, MA 02138, USA

Received 21 August 2006 / Received in final form 10 October 2006

Published online 15 November 2006 – © EDP Sciences, Società Italiana di Fisica, Springer-Verlag 2006

Abstract. We investigate the time evolution of entanglement for bipartite systems of arbitrary dimensions under the influence of decoherence. For qubits, we determine the precise entanglement decay rates under different system-environment couplings, including finite temperature effects. For qudits, we show how to obtain upper bounds for the decay rates and also present exact solutions for various classes of states.

PACS. 03.67.-a Quantum information – 03.67.Mn Entanglement production, characterization, and manipulation – 03.65.Yz Decoherence; open systems; quantum statistical methods

QICS. 02.40.+d Interaction with environment and decoherence – 03.40.+t Thermal/mixed state entanglement – 03.10.+m Entanglement measures

1 Introduction

The production of entangled states and the control of their time evolution became a major issue in current research in view of the development of quantum information theory, and all possible applications associated with it. Besides the formidable experimental advances in this direction, there remains a main obstacle which is the fragility of entanglement under the unavoidable interaction with the environment. This coupling of the quantum system with its surroundings, and the consequent decay of entanglement, motivates important questions such as to understand its sources, to identify the characteristic timescales, and, possibly, to find ways to circumvent it.

To devise appropriate strategies for controlling entangled states under the effect of environment interaction, the first step is to acquire a deeper understanding of the dynamics of the decoherence processes themselves. Despite the rapidly increasing experimental interest in this subject, due to the possibility of monitoring entanglement dynamics [1], most of the theoretical work focused on characterizing static properties of entanglement for quantum states [2–5].

Only very recently the question of entanglement decay under environment-induced mixing has been addressed, for some specific states and environment models, and restricted to the case of two qubits [6–11], probably due to the lack of a genuine *and* computable entanglement mea-

sure for systems larger than that. Nonetheless, new techniques for the derivation of bounds [12,13] of concurrence, one possible entanglement measure, recently allowed a systematic study of entanglement dynamics for more general states, including multipartite [14,15] and multi-level systems.

These higher dimensional systems are of great interest since they can enlarge the perspectives of efficient applications in quantum information and can also be used to test fundamental aspects of quantum theory. In fact, entangled states of two d -dimensional quantum systems, the *qudits*, can improve measurement resolution [16,17] and are known to violate local realism more strongly than qubits [18,19]. Moreover, they can be used for quantum computation [20–23] and also in quantum cryptography protocols [24,25], which are safer [26,27] than their qubit counterparts. Despite the importance of such entangled qudits, reflected in the intense activity on their production and manipulation in different experimental setups [28–34], their dynamics under the influence of environment interaction remained unexplored until now.

The paper is organized as follows. In Section 2 we will briefly recall a recently developed approach for calculating concurrence which allows us to investigate entanglement between systems of arbitrary dimensions. In Section 3 we will present the different models which describe the interaction of the system with the environment. Section 4 is devoted to the analysis of the entanglement decay rates under decoherence processes, starting from the case of bipartite qubits. With the available analytical tools, some,

^a e-mail: andre.carvalho@anu.edu.au

still unknown, features of the decoherence dynamics are presented. The section closes with the analysis of bipartite qudits. A summary of the main results of the paper is presented in the concluding Section 5.

2 Entanglement measure: concurrence

In order to follow the environment-induced time evolution of entanglement, one needs a measure which satisfactorily deals with mixed states. A commonly used measure in the context of two qubits is the concurrence [35], defined for pure states as

$$c(\Psi) = \left| \langle \Psi^* | \sigma_y \otimes \sigma_y | \Psi \rangle \right|, \quad (1)$$

where $*$ stands for complex conjugation performed in the standard, computational basis. For mixed states it can be formulated as

$$c(\rho) = \inf_{\{p_i, \Psi_i\}} \sum_i p_i c(\Psi_i), \quad (2)$$

with

$$p_i > 0, \text{ and } \rho = \sum_i p_i |\Psi_i\rangle \langle \Psi_i|. \quad (3)$$

In contrast to most other measures, equation (2) can be solved algebraically with the well known solution $c(\rho) = \max\{\lambda_1 - \lambda_2 - \lambda_3 - \lambda_4, 0\}$, in terms of the square roots, λ_i , of the decreasingly ordered eigenvalues of the matrix $\rho(\sigma_y \otimes \sigma_y) \rho^* (\sigma_y \otimes \sigma_y)$.

For higher dimensional systems, we will use the generalization of concurrence given in [36] that coincides — though not obviously — with the original concurrence [35] if restricted to two-level systems. For practical purposes, it is convenient to express concurrence [37,38] in terms of an operator A acting on the product space $\mathcal{H} \otimes \mathcal{H}$ of two copies of the system, as

$$c(\Psi) = \sqrt{\langle \Psi | \otimes \langle \Psi | A | \Psi \rangle \otimes | \Psi \rangle}. \quad (4)$$

The operator

$$A = \sum_{\alpha} |\chi_{\alpha}\rangle \langle \chi_{\alpha}| \quad (5)$$

is the projector onto the space spanned by the states $|\chi_{\alpha}\rangle$ that are anti-symmetric with respect to the exchange of the copies of either \mathcal{H}_1 or \mathcal{H}_2 , i.e.

$$|\chi_{\alpha}\rangle = (|i_k i_l\rangle - |i_l i_k\rangle) \otimes (|j_m j_n\rangle - |j_n j_m\rangle). \quad (6)$$

The states $\{|i_k\rangle\}$ and $\{|j_m\rangle\}$ form, respectively, arbitrary local bases of \mathcal{H}_1 and \mathcal{H}_2 , and α is a label for the multi-index $[k, l, m, n]$.

To extend this construction for the case of mixed states, one should substitute equation (4) in the convex-roof, equation (2), which can be written, in terms of subnormalized states $|\psi_i\rangle = \sqrt{p_i} |\Psi_i\rangle$, as

$$c(\rho) = \inf_{\{\psi_i\}} \sum_i \sqrt{\langle \psi_i | \otimes \langle \psi_i | A | \psi_i \rangle \otimes | \psi_i \rangle}. \quad (7)$$

Unfortunately, apart from the two-level case where the operator A can be written in terms of a single vector $|\chi\rangle = (|01\rangle - |10\rangle) \otimes (|01\rangle - |10\rangle)$, no exact solutions for equations (2) and (7) are known and, hence, one has to rely on numerical efforts to calculate the concurrence. Also note that numerical solutions of this optimization procedure define only an upper bound for concurrence, since there is no a priori information available on whether the global minimum or just a local one has been reached.

To circumvent this problem, we will use suitable approximations which provide lower bounds of concurrence [12,13] and not only allow for an efficient numerical approach, but also, in some cases, for exact algebraic solutions. Starting from a decomposition of the density matrix in terms of pure (subnormalized) states $\rho = \sum_i |\phi_i\rangle \langle \phi_i|$ and from the vectors $|\chi_{\alpha}\rangle$, one can define a set of matrices T^{α} , given by¹

$$T_{jk}^{\alpha} = \langle \chi_{\alpha} | \phi_j \rangle \otimes | \phi_k \rangle. \quad (8)$$

These are connected to the previously defined operator A through the tensor

$$\mathcal{A}_{jk}^{lm} = \sum_{\alpha} (T_{lm}^{\alpha})^* T_{jk}^{\alpha} = \langle \psi_l | \otimes \langle \psi_m | A | \psi_j \rangle \otimes | \psi_k \rangle. \quad (9)$$

It was shown in [12] that concurrence is bounded from below by

$$c(\rho) \geq \max \left\{ \mathcal{S}_1 - \sum_{i>1} \mathcal{S}_i, 0 \right\}, \quad (10)$$

where the \mathcal{S}_i are the decreasingly ordered singular values of

$$\mathcal{T} = \sum_{\alpha} Z_{\alpha} T^{\alpha}, \text{ with } \sum_{\alpha} |Z_{\alpha}|^2 = 1, \quad (11)$$

that still depend on the choice of the complex parameters Z_{α} . Although any choice provides a lower bound, one might still wish to carry out an optimization over Z_{α} , though now on a much smaller parameter space and with simpler constraints than in equation (7). Moreover, also each matrix T^{α} already provides a lower bound, which can be calculated algebraically.

Finally, let us describe an experimentally motivated approach to calculate lower bounds of concurrence, the quasi-pure approximation [13]. Although environmental influences cannot be avoided completely, under typical experimental conditions one deals with states which are, at least initially, *quasi-pure*. This is, they have a single eigenvalue μ_1 which is much larger than all the others, and an approximation based on this condition can be developed. Indeed, using the spectral decomposition $\rho = \sum_i \mu_i |\Psi_i\rangle \langle \Psi_i|$ of the density matrix and the previously defined subnormalized states, one can see that the elements of \mathcal{A} defined in equation (9) are proportional to the square roots of the eigenvalues μ_i :

$$\mathcal{A}_{jk}^{lm} \propto \sqrt{\mu_j \mu_k \mu_l \mu_m}. \quad (12)$$

¹ Note that $|\chi_{\alpha}\rangle \in \mathcal{H}_1 \otimes \mathcal{H}_1 \otimes \mathcal{H}_2 \otimes \mathcal{H}_2$, whereas $|\phi_j\rangle \otimes |\phi_k\rangle \in \mathcal{H}_1 \otimes \mathcal{H}_2 \otimes \mathcal{H}_1 \otimes \mathcal{H}_2$. Nevertheless, the two spaces are isomorphic, and it is straightforward to identify the correspondence between their elements.

This proportionality and the assumption that $\mu_1 \gg \mu_i$ allows to order the elements of \mathcal{A} in powers of the square roots of μ_i . Keeping only the leading order terms, i.e., \mathcal{A}_{11}^{11} at zero order, \mathcal{A}_{11}^{j1} , \mathcal{A}_{11}^{1j} , \mathcal{A}_{j1}^{11} and \mathcal{A}_{1j}^{11} at first order, and so on, we can approximate \mathcal{A} by

$$\mathcal{A}_{jk}^{lm} \simeq (T_{lm}^{(\text{qp})})^* T_{jk}^{(\text{qp})}, \quad (13)$$

with

$$T_{jk}^{(\text{qp})} = \frac{\mathcal{A}_{jk}^{11}}{\sqrt{\mathcal{A}_{11}^{11}}}. \quad (14)$$

Thus the quasi-pure concurrence can be written as

$$c(\rho) \simeq c_{\text{qp}}(\rho) = \max \left\{ \mathcal{S}_1 - \sum_{i>1} \mathcal{S}_i, 0 \right\}, \quad (15)$$

where the \mathcal{S}_i are the singular values of the matrix $T^{(\text{qp})}$ defined in equation (14).

With these tools at hand, entanglement in higher dimensional systems can be explored in a computationally manageable way. We will use them to monitor the entanglement dynamics under different sources of decoherence.

3 Environment models

We are considering composite quantum systems with constituents separated by distances large enough to assume that an excitation emitted by one subsystem to the environment will never be absorbed by another subsystem. This is typically the case in experiments with trapped ions or atoms, where is therefore legitimate to assume that each subsystem interacts only, and independently, with its local environment. The dynamics under such decoherence process can be described by the master equation

$$\frac{d\rho}{dt} = (\mathbb{1} \otimes \mathcal{L} + \mathcal{L} \otimes \mathbb{1}) \rho, \quad (16)$$

where ρ is the reduced density operator of the system. Since all subsystems are of the same kind, e.g. atoms or ions of the same isotope, the interactions of each component of the system with the environment are of the same form, represented by the same local Lindblad operator \mathcal{L} . Under the — in typical experiments well justified — assumption of Markovian dynamics, and the fundamental requirement of complete positivity, the action of \mathcal{L} on ρ reads

$$\mathcal{L}\rho = \sum_i \frac{\Gamma_i}{2} \left(2L_i \rho L_i^\dagger - L_i^\dagger L_i \rho - \rho L_i^\dagger L_i \right). \quad (17)$$

The operators L_i and the rates Γ_i are determined by the underlying coupling mechanisms of a specific experiment. Though, the very general form of equation (17) allows to describe various physical situations, such as dissipation of systems with higher effective temperature than that of the environment, or heating in the opposite case. But also

the mere loss of phase can be described within the same framework.

For two-level systems, the operators L_i can be written in terms of the Pauli matrices. In the case of an interaction with a thermal bath, the Lindblad operator reads

$$\mathcal{L}\rho = \frac{\Gamma(\bar{n}+1)}{2} (2\sigma_- \rho \sigma_+ - \sigma_+ \sigma_- \rho - \rho \sigma_+ \sigma_-) + \frac{\Gamma\bar{n}}{2} (2\sigma_+ \rho \sigma_- - \sigma_- \sigma_+ \rho - \rho \sigma_- \sigma_+). \quad (18)$$

In this equation, the first and the second term on the right hand side describe, respectively, decay and excitation processes (mediated by the two-level excitation and deexcitation operators σ_+ and σ_-), with rates which depend on the temperature, here parametrized by \bar{n} , the average thermal excitation of the reservoir. In the zero temperature limit, $\bar{n} = 0$, only the spontaneous decay term survives, leading to a purely dissipative process, which corresponds to the fundamental limiting factor for the coherent evolution of atomic qubits. Noisy dynamics corresponds to the infinite temperature limit, where $\bar{n} \rightarrow \infty$, and, simultaneously, $\Gamma \rightarrow 0$, so that $\Gamma\bar{n} \equiv \tilde{\Gamma}$ is constant. In this case, decay and excitation occur at exactly the same rate, and the noise induced by the transitions between the two levels brings the system to a stationary, maximally mixed state. Finally, a purely dephasing reservoir is obtained by choosing $L_i = d = \sigma_+ \sigma_-$, leading to the master equation

$$\frac{d\rho}{dt} = \frac{\Gamma}{2} (2\sigma_+ \sigma_- \rho \sigma_+ \sigma_- - \sigma_+ \sigma_- \rho - \rho \sigma_+ \sigma_-). \quad (19)$$

In this case, only the off-diagonal elements of the density matrix decay, and phase coherence is lost. This dephasing mechanism is known to be an important source of decoherence in ion traps [39, 40] and in quantum dot experiments [41–43].

If we consider a system of qudits, the operators L_i in equation (17) cannot be written anymore in terms of Pauli matrices. To describe the effect of the environment in such systems, we will consider the qudits as two bosonic modes, with an equidistant spectrum, and truncated bases of length d . The terms n and m in the general (pure) state $|\psi\rangle = \sum_{n,m=0}^{d-1} \psi_{nm} |nm\rangle$ then indicate the occupation number in each of these modes. Decay and excitation processes now correspond to the action of annihilation and creation operators a and a^\dagger , analogous to the σ_- and σ_+ for qubits. With this convention, the thermal and dephasing environments are described, respectively, by

$$\mathcal{L}\rho = \frac{\Gamma(\bar{n}+1)}{2} (2a\rho a^\dagger - a^\dagger a \rho - \rho a^\dagger a) + \frac{\Gamma\bar{n}}{2} (2a^\dagger \rho a - a a^\dagger \rho - \rho a a^\dagger), \quad (20)$$

and

$$\mathcal{L}\rho = \frac{\Gamma}{2} (2a^\dagger a \rho a^\dagger a - a^\dagger a \rho - \rho a^\dagger a). \quad (21)$$

Zero and infinite temperature limits are obtained as in the qubit case, and represent, to a very good approximation, the decoherence processes of photons in high- Q

cavities [44], and of motional degrees of freedom in ion traps [45].

4 Entanglement dynamics under decoherence

4.1 Two qubits case

We shall begin our analysis with the case of two qubits, since it allows for analytical solutions, and can provide some intuition of the processes at work in higher dimensional systems. To provide a more complete and systematic description of the time scales of entanglement decay under environment interaction, we will recall some known results for the case of dephasing and zero temperature reservoirs, and furthermore derive exact solutions when finite temperature effects are taken into account.

Let us start with initially prepared Bell states $|\Psi^\pm\rangle = (|01\rangle \pm |10\rangle)/\sqrt{2}$, and $|\Phi^\pm\rangle = (|00\rangle \pm |11\rangle)/\sqrt{2}$. Their concurrences as a function of time are given by

$$c(\Psi^\pm, t) = c(\Phi^\pm, t) = e^{-\Gamma t}, \quad (22)$$

for the dephasing environment, and by

$$c(\Psi^\pm, t) = e^{-\Gamma t}, \quad c(\Phi^\pm, t) = e^{-2\Gamma t}, \quad (23)$$

for the zero temperature case. The first important observation is the accelerated (by a factor of two) decay of concurrence for the Φ^\pm as compared to the Ψ^\pm states, under the influence of a zero temperature environment. This can be understood from the time scales involved in the corresponding solution for the density matrix: while for Ψ^\pm each term $|01\rangle$ and $|10\rangle$ corresponds to a single particle decay, leading to a time scale $e^{-\Gamma t}$, we have the term $|11\rangle$ in Φ^\pm , such that both particles can undergo an environment induced transition to the ground state, thus introducing a faster, $e^{-2\Gamma t}$, decay.

Also for the finite temperature case an explicit solution be calculated for initial Bell states: it reads

$$c(t) = \max\{c_T(t), 0\}, \quad (24)$$

where the function $c_T(t)$, for Ψ^\pm and Φ^\pm states, is given, respectively, by

$$c_T(\Psi^\pm, t) = \beta - \frac{2(1-\beta)\sqrt{(\bar{n}^2 + \bar{n})^2(\beta+1)^2 + \beta(\bar{n}^2 + \bar{n})}}{(2\bar{n}+1)^2}, \quad (25)$$

and

$$c_T(\Phi^\pm, t) = \beta + \frac{[2\bar{n}(\bar{n}+1) + 1]\beta^2 - \beta - 2\bar{n}(\bar{n}+1)}{(2\bar{n}+1)^2}, \quad (26)$$

with $\beta = e^{-\Gamma(2\bar{n}+1)t}$. These expressions, which reveal the precise role of temperature on the decay of entanglement of Bell states, show that, distinct from the cases of dephasing and zero temperature environments, concurrence

does not decay according to a simple mono-exponential law, but rather exhibits various time scales.

To apprehend the essential features of temperature effects on entanglement decay, it is useful to focus on the short time limit of these equations [46]. Expanding equations (25) and (26) to first order in t , one finds that the short time concurrence decay is given by

$$c(\Psi^\pm, t) \simeq 1 - \left(2\bar{n} + 1 + 2\sqrt{\bar{n}(\bar{n}+1)}\right) \Gamma t, \quad (27)$$

and

$$c(\Phi^\pm, t) \simeq 1 - 2(2\bar{n} + 1)\Gamma t. \quad (28)$$

This shows that, at the beginning of the evolution, a finite temperature reservoir increases the concurrence decay rate, as compared to the zero temperature case, by a factor of $\left(2\bar{n} + 1 + 2\sqrt{\bar{n}(\bar{n}+1)}\right)$ and of $(2\bar{n} + 1)$, for Ψ^\pm and Φ^\pm states, respectively.

From equations (25) and (26), one can also derive the infinite temperature limit ($\bar{n} \rightarrow \infty$, $\Gamma \rightarrow 0$, with $\Gamma\bar{n} \equiv \tilde{\Gamma} = \text{const.}$) of the thermal bath. In this case, the concurrence becomes

$$c(\Psi^\pm, t) = c(\Phi^\pm, t) = \max\left\{\frac{e^{-4\tilde{\Gamma}t}}{2} + e^{-2\tilde{\Gamma}t} - \frac{1}{2}, 0\right\}. \quad (29)$$

Note that, again, entanglement dynamics involves different time scales. However, a single exponential captures the basic behavior of entanglement decay, since equation (29) can be well fitted by a function in the form $\alpha e^{-\gamma t} + \delta$, with negative offset δ . Consequently, separability, i.e. $c(t) = 0$, is reached at finite times for the infinite temperature environment, as well as for any $\bar{n} > 0$. This is in contrast to the above dephasing and zero temperature environments, where separability is reached only asymptotically, and follows from the long-time limit for $c_T(t)$ in equation (24)

$$\lim_{t \rightarrow \infty} c_T(t) = -\frac{2\bar{n}(\bar{n}+1)}{(2\bar{n}+1)^2}, \quad (30)$$

which is non-positive for all $\bar{n} > 0$. The exact expressions for this separability time can be easily obtained from the condition $c(t) = 0$, and are of the form

$$t_{\text{sep}} = \ln[f(\bar{n})]/\Gamma(2\bar{n}+1),$$

where the function $f(\bar{n})$ depends on the initial state Ψ^\pm or Φ^\pm . Observe, however, that this is not true for arbitrary initial states. Indeed, some initially mixed states [9] as well as some pure non-maximally entangled states, e.g., $|\psi\rangle = \frac{1}{2}|00\rangle + \frac{1}{2}|01\rangle + \frac{1}{\sqrt{2}}|11\rangle$, reach separability on finite time scales even for a zero temperature environment.

4.2 Two qudits case

As the dimensions of the subsystems increase, not only a general analytical solution is unknown, but also the numerical approach to obtain reliable estimates of concurrence rapidly turns into a very demanding task. However,

it is exactly in this situation where the strength of the tools derived in Section 2, for calculating lower bounds of concurrence, becomes manifest. We will devote the remainder of this paper to a systematic analysis of entanglement dynamics in bipartite qudits, using these tools. In particular, we will extract bounds for the *decay rates* of entanglement, and also show how one can infer analytical solutions even for arbitrary dimensions, from the knowledge of the dynamics of the system.

4.2.1 Dephasing environment: an exactly solvable example

We begin our analysis with the dephasing dynamics described by equation (21), which, as discussed in Section 3, induces a decay of the off-diagonal elements of the density matrix without changing the diagonal ones. Besides its importance in the description of different physical situations, as already mentioned before, the dephasing model is very instructive since it allows for obtaining analytical solutions for the concurrence of some classes of states.

Let us first assume that the initial pure state is of the form $|\psi\rangle = a|m_1m_2\rangle + b|n_1n_2\rangle$, what comprises two-level Bell states as special cases. In this situation, one can write the solution of equation (21) as

$$\rho(t) = |a|^2|m_1m_2\rangle\langle m_1m_2| + |b|^2|n_1n_2\rangle\langle n_1n_2| + e^{-\gamma t}ab^*|m_1m_2\rangle\langle n_1n_2| + e^{-\gamma t}a^*b|n_1n_2\rangle\langle m_1m_2|, \quad (31)$$

with

$$\gamma = \frac{\Gamma}{2} [(m_1 - n_1)^2 + (m_2 - n_2)^2]. \quad (32)$$

(Note that pure dephasing does not decrease the average excitation of the system.) There is just one decaying element (and its conjugate) in the density matrix evolution and, therefore, one expects that the entanglement decay rates should follow the same behavior. This is indeed the case, as we will show using the techniques described in Section 2: first, one can easily check that the mixed state (31) can be decomposed into contributions of two pure states,

$$|\phi_1\rangle = \sqrt{p}(a|m_1m_2\rangle + b|n_1n_2\rangle), \quad (33)$$

and

$$|\phi_2\rangle = \sqrt{1-p}(a|m_1m_2\rangle - b|n_1n_2\rangle), \quad (34)$$

with $p = (1 + e^{-\gamma t})/2$, and $\rho = |\phi_1\rangle\langle\phi_1| + |\phi_2\rangle\langle\phi_2|$. From the structure of this decomposition, one can see that, among all $|\chi_\alpha\rangle$, only $|\chi\rangle = (|m_1n_1\rangle - |n_1m_1\rangle) \otimes (|m_2n_2\rangle - |n_2m_2\rangle)$ gives a non-zero contribution for T^α in equation (8). In this case, the concurrence can be expressed in terms of a single matrix T , which reads

$$T = \begin{pmatrix} 2pab & 0 \\ 0 & 2(p-1)ab \end{pmatrix}.$$

Thus the formal structure of two-level systems is retrieved, and the lower bound, equations (10) and (11), is exact.

From the singular values of the matrix T , one readily obtains

$$c(t) = 2|ab|e^{(-\Gamma t/2)[(m_1-n_1)^2+(m_2-n_2)^2]}, \quad (35)$$

which is equal to the sum of the absolute values of the two non-vanishing off-diagonal elements of $\rho(t)$.

4.2.2 Zero temperature environment: exact solutions, and estimates

Although there are no a priori criteria from which to infer the existence of exact solutions like equation (35) in general, this is still possible for a large variety of physical situations. For a zero temperature environment, for example, exact solutions can be derived based on a given form of the decomposition of ρ . Moreover, even if such decomposition does not exist, it is still possible to obtain estimates on the decay rates of concurrence with the tools described in Section 2.

To illustrate this, we start with states of the form $|\psi\rangle = a|0m\rangle + b|m0\rangle$ and consider, for the derivation of the exact solution, the case of three-level systems and $a = b = 1/\sqrt{2}$. The decomposition of $\rho(t)$ in terms of its eigenstates (with non-vanishing eigenvalues) reads

$$|\phi_1\rangle = e^{-\Gamma t} (|02\rangle + |20\rangle) / \sqrt{2} \quad (36)$$

$$|\phi_2\rangle = \sqrt{e^{-\Gamma t} (1 - e^{-\Gamma t})} |01\rangle, \quad (37)$$

$$|\phi_3\rangle = \sqrt{e^{-\Gamma t} (1 - e^{-\Gamma t})} |10\rangle, \quad (38)$$

and

$$|\phi_4\rangle = (1 - e^{-\Gamma t}) |00\rangle. \quad (39)$$

All these states, with the exception of $|\phi_1\rangle$, are separable. Therefore, from equation (2), one can see that the concurrence of $|\phi_1\rangle$ is an upper bound of $c(\rho)$. Moreover, this term is also the only one that gives a non-vanishing contribution to the matrix $T^{(\text{qp})}$, equation (14), in the quasi-pure approximation. Hence, lower and upper bounds coincide and the solution $c(t) = e^{-2\Gamma t}$ is exact. For the state $|\psi\rangle = a|0m\rangle + b|m0\rangle$ the demonstration is analogous, and the concurrence is given by

$$c(t) = 2|ab|e^{-m\Gamma t}. \quad (40)$$

From the time-dependent matrix elements of ρ , which can be obtained from equation (20) with $\bar{n} = 0$, one can see that, as in equation (35), concurrence is simply given by the sum of the absolute values of the only two non-vanishing off-diagonal elements of ρ . However, we should emphasize that this only happens in special cases alike the present one and, in general, there is no simple relation between the decay of off-diagonal elements of ρ and concurrence.

An example where such a simple relation does not exist, even though an exact solution is possible, is the zero temperature dynamics of initial states of the form

$|\psi\rangle = a|00\rangle + b|mm\rangle$. The time-dependent density matrix can be decomposed as $\rho = \xi + \eta$, with η diagonal in the $\{|ij\rangle\}$ basis (and thus separable), and $\xi = \sum \langle ij|\rho|pq\rangle |ij\rangle\langle pq|$ with $i, j, p, q \in \{0, m\}$. From this argument and from equation (2) it follows that the concurrence of ξ is an upper bound of $c(\rho)$. Furthermore, ξ is a two-qubit-like matrix and its concurrence can be readily obtained as

$$c(t) = 2e^{-m\Gamma t} \left(|ab| - (1 - e^{-\Gamma t})^m |b|^2 \right). \quad (41)$$

This result coincides with the quasi-pure approximation of $c(\xi)$, calculated using $|\chi\rangle = (|0m\rangle - |m0\rangle) \otimes (|0m\rangle - |m0\rangle)$ in equations (8, 9, 15), and hence is exact.

It is clear from equation (41) that the entanglement decay, in this case, encompasses different time scales for $d > 2$, while the only non-zero off-diagonal elements, $\langle 00|\rho|mm\rangle$ and $\langle mm|\rho|00\rangle$, decay as $e^{-m\Gamma t}$. Note also that, in the limit of large m , the concurrence tends to $c(t) = 2|ab|e^{-m\Gamma t}$ and then coincides with the result of equation (40). Thus, in this limit, the state $|\psi\rangle = a|00\rangle + b|mm\rangle$ decays as the state $|\psi\rangle = a|0m\rangle + b|m0\rangle$. This shows that the robustness of the Ψ^\pm Bell states as compared to the Φ^\pm in terms of decay rates in the two qubit case (see Eq. (23)) fades away for larger dimensions.

In the two previous examples, exact solutions were possible because ρ could be decomposed into a separable part, and a non-separable two-level-like complement, for which upper and lower bounds coincide. Although, at first sight, one might judge these conditions to be rather restrictive, the above considerations can also be applied to other environment models and qubit-like initial states. However, what happens when such decomposition does not exist? How much information on the decay rates can we extract with the available tools?

To help to answer these questions let us focus on the situation shown in Figure 1, where an analytical solution could not be found. For the initial state $|\psi\rangle = (|12\rangle + |21\rangle)/\sqrt{2}$, upper (2) and optimized lower bounds (10, 11), as well as quasi-pure calculations (15), are presented in the upper panel of the figure, as circles, crosses, and squares, respectively. The solid lines represent the quasi-pure approximations for initial states of the form $|\psi\rangle = (|1m\rangle + |m1\rangle)/\sqrt{2}$, with $m = d - 1$ and, from top to bottom, $d = 4$ to $d = 7$. Note that the quasi-pure approximations are calculated only until times when the initially largest eigenvalue λ_1 coincides with the second one (see the lower panel of Fig. 1 for the case $d = 3$). The quasi-pure solutions exhibit a simple time dependence $e^{-(m+1)\Gamma t}$. For $d = 3$, we can go further and use also the numerically calculated upper bound, which in this case is found (through curve fitting) to behave as $e^{-2\Gamma t}$, to confine the actual value of the decay rate to the interval $2\Gamma \leq \gamma \leq 3\Gamma$. Furthermore, we can state that, for arbitrary dimensions, the decay rate cannot exceed the value given by the quasi-pure approximation, which, in the present case, leads to $\gamma \leq \Gamma d$. This is a noticeable asset of our analysis. Even if the high dimension of the system, together with the complex structure of the states, does not allow to determine the precise decay rates of

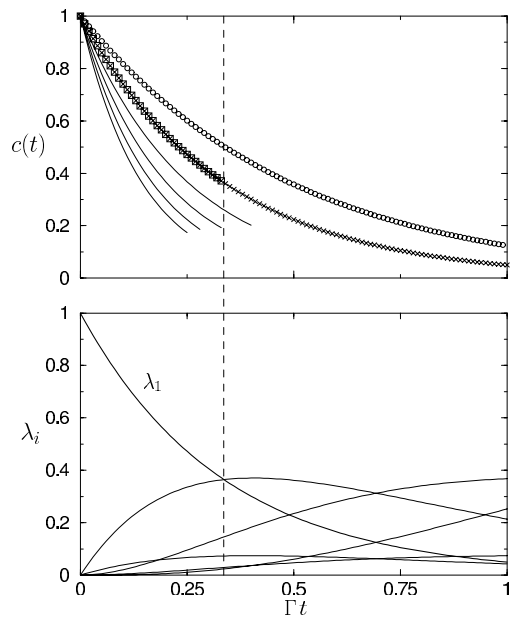


Fig. 1. Top panel: optimized upper (circles) and lower (crosses) bounds of concurrence, as well as quasi-pure approximation (squares), for the initial state $|\psi\rangle = (|12\rangle + |21\rangle)/\sqrt{2}$ coupled to a zero temperature reservoir. The solid lines show the quasi-pure approximations for initial states $|\psi\rangle = (|1m\rangle + |m1\rangle)/\sqrt{2}$, with $m = d - 1$ and, from top to bottom, $d = 4$ to $d = 7$. Quasi-pure solutions behave as $e^{-(m+1)\Gamma t}$, and the upper bound for $d = 3$ is correctly fitted by $e^{-2\Gamma t}$. Bottom panel: eigenvalues of the density matrix $\rho(t)$ as a function of time, for $d = 3$. Quasi-pure results coincide with the optimized lower bound, and are indicated only for times during which λ_1 remains the largest eigenvalue.

entanglement in the general case, we can extract useful information on their bounds.

4.2.3 Decay of maximally entangled states

In the previous two sections, we described how the entanglement of some classes of states decay under dephasing and damping environments. The particularly simple forms of those states were useful not only to demonstrate the potential of our approach, but also to allow for a direct comparison with the decay of two qubits. All the initial qudit states considered so far have the same amount of entanglement as a Bell state, but the possibility of exploring the higher dimensionality induces a faster decay, as shown by equations (35, 40), and (41). Therefore, from the point of view of fragility of entanglement, our results show that the above classes of states cannot outperform the slowest decaying Bell state.

However, to be fair with higher dimensional systems, one should consider not only the undesirable effect of increase in the decay rates, but also the benefit of possibly having a larger amount of entanglement in the initial state. For this purpose, we analyzed the dynamics of maximally

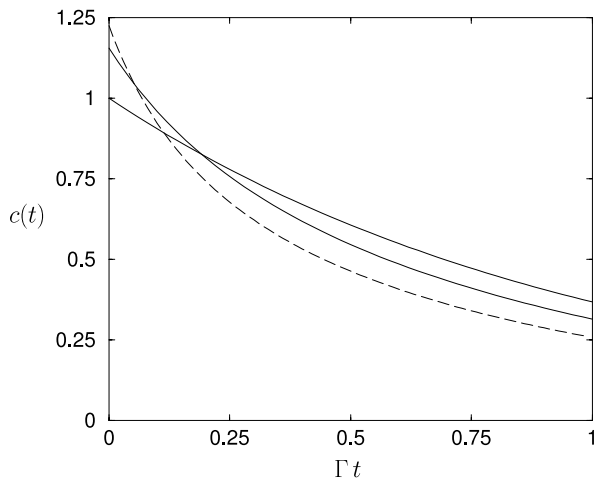


Fig. 2. Concurrence decay for maximally entangled initial states $|\psi\rangle_{\text{me}}$, equation (42), under a dephasing reservoir. The bold solid line shows concurrence for $d = 2$, while solid and dashed lines correspond to the quasi-pure approximation for $d = 3$ and $d = 4$, respectively. Larger amounts of entanglement inscribed in a higher dimensional initial state need to be harvested immediately, since they quickly fade away.

entangled initial states

$$|\psi\rangle_{\text{me}} = \frac{1}{\sqrt{d}} \sum_{k=0}^{d-1} |kk\rangle, \quad (42)$$

and compared their decay for different dimensions.

In Figure 2 we show the time evolution of the quasi-pure approximation for $|\psi\rangle_{\text{me}}$ in $d = 2$ (bold solid line), $d = 3$ (solid line), and $d = 4$ (dashed line), for a dephasing environment (for the zero temperature case the situation is similar). Apparently, there is a trade-off between the increase in the initial entanglement and the enhanced decay rates, both provided by higher dimensionality. For $t = 0$, which corresponds to the idealized case of pure maximally entangled states, it is always advantageous to increase the dimensionality, and, consequently, the entanglement. However, already in the presence of dephasing, this gain is ruined after some time, showing that the use of the states $|\psi\rangle_{\text{me}}$ in higher dimensions is only favourable for $\Gamma t \ll 1$, i.e., for weak coupling or short times.

4.2.4 Finite temperature environment

Finally, let us briefly present a situation where the ability to handle higher dimensional systems is essential: the finite temperature reservoir. Any initial state will evolve asymptotically into a thermal state, which can be described by a finite number of levels. This number however increases with temperature.

The decoherence effect of such environment on qudits is illustrated in Figure 3, for an initial state $|\psi\rangle = (|01\rangle + |10\rangle)/\sqrt{2}$. The solid, dashed and long-dashed lines represent, respectively, the two-qubit solution, equation (25),

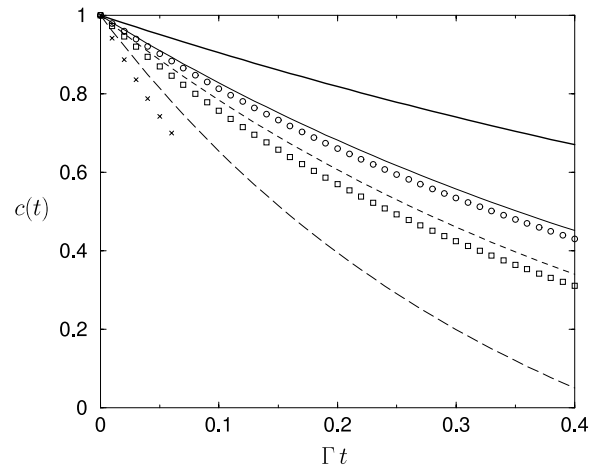


Fig. 3. Finite temperature effects on the decay of entanglement, for an initial Bell state Ψ^+ . Solid, dashed and long dashed lines indicate, respectively, the two-level case solutions of equation (18), given by equation (25), for $\bar{n} = 0.1$, $\bar{n} = 0.2$, and the infinite temperature limit. Circles, squares and crosses show the corresponding quasi-pure results for the qudits' dynamics given by equation (20), using a truncated basis with $d = 8$. For comparison, also the solution for a zero temperature environment is shown (bold line). The expected enhancement of the decay rates with increasing temperature is more pronounced in the higher dimensional case.

for $\bar{n} = 0.1$, $\bar{n} = 0.2$, and the infinite temperature limit. The corresponding quasi-pure estimates for the same initial state evolving under equation (20) are given by circles, squares and crosses. The bold solid curve indicates, for comparison, the zero temperature evolution. The dimension used in the simulations ($d = 8$) was chosen to be large enough to describe the dynamics of the system for $\bar{n} = 0.1$ and $\bar{n} = 0.2$, for the times considered in the figure. Note that for the infinite temperature case actually an infinite basis is needed, and that our truncated basis set allows for a correct description of the dynamics only for a short period of time ($\bar{\Gamma}t \approx 0.06$), as long as the dynamics do not populate levels at the boundary of the Hilbert space.

The most noticeable effect here is that the expected enhancement of the decay rates with temperature is more pronounced for qudits than for qubits. As a matter of fact, this is not too surprising since the dynamics of a finite temperature bath, given by equation (20), induces transitions to many different levels, thus speeding up entanglement decay.

5 Conclusions

The present paper contributes to the understanding of entanglement dynamics under environment coupling, for two qudit-systems. Although no analytical solutions are available in general, we have shown that they can be obtained for different classes of initial states and dynamics. Moreover, we have shown how suitable decompositions of

the density matrix, together with methods for calculating lower bounds of concurrence, can be useful to decide on the existence of exact solutions and to derive them for concurrence or its lower bounds. For more general cases in high dimensional systems, we were able to derive upper bounds for the decay rates of entanglement.

Using the above techniques were able to estimate, and in some cases exactly derive, the time scales for entanglement decay in multi-level systems. Our results shows that decay rates for qudits are not only larger than the corresponding qubit ones, but also more sensitive to finite temperature effects. We have also shown that the advantage of increasing dimensionality to obtain higher entanglement for pure states is rapidly suppressed when environment interactions are taken into account. The use of maximally entangled states in higher dimensions is therefore only justified in the case of weak coupling, or for short times.

Future work will focus on error estimates for the employed estimates of concurrence in higher dimensions.

References

1. C.F. Roos, G.P.T. Lancaster, M. Riebe, H. Häffner, W. Hänsel, S. Gulde, C. Becher, J. Eschner, F. Schmidt-Kaler, R. Blatt, *Phys. Rev. Lett.* **92**, 220402 (2004)
2. C.H. Bennett, H.J. Bernstein, S. Popescu, B. Schumacher, *Phys. Rev. A* **53**, 2046 (1996)
3. C.H. Bennett, D.P. DiVincenzo, J.A. Smolin, W.K. Wootters, *Phys. Rev. A* **54**, 3824 (1996)
4. G. Vidal, *J. Mod. Opt.* **47**, 355 (2000)
5. G. Vidal, R.F. Werner, *Phys. Rev. A* **65**, 032314 (2002)
6. K. Życzowski, P. Horodecki, M. Horodecki, R. Horodecki, *Phys. Rev. A* **65**, 012101 (2001)
7. T. Yu, J.H. Eberly, *Phys. Rev. B* **66**, 193306 (2002)
8. T. Yu, J.H. Eberly, *Phys. Rev. B* **68**, 165322 (2003)
9. T. Yu, J.H. Eberly, *Phys. Rev. Lett.* **93**, 140404 (2004)
10. M. Ziman, V. Buzek, *Phys. Rev. A* **72**, 052325 (2005)
11. C. Pineda, T.H. Seligman, e-print [arXiv:quant-ph/0605169](https://arxiv.org/abs/quant-ph/0605169) (2006)
12. F. Mintert, M. Kuś, A. Buchleitner, *Phys. Rev. Lett.* **92**, 167902 (2004)
13. F. Mintert, A. Buchleitner, *Phys. Rev. A* **72**, 012336 (2005)
14. A.R.R. Carvalho, F. Mintert, A. Buchleitner, *Phys. Rev. Lett.* **93**, 230501 (2004)
15. X.S. Ma, A. Wang, X.D. Yang, F. Xu, *Eur. Phys. J. D* **37**, 135 (2006)
16. M.W. Mitchell, J.S. Lundeen, A.M. Steinberg, *Nature* **429**, 161 (2004)
17. A.N. Boto, P. Kok, D.S. Abrams, S.L. Braunstein, C.P. Williams, J.P. Dowling, *Phys. Rev. Lett.* **85**, 2733 (2000)
18. D. Kaszlikowski, P. Gnaniński, M. Żukowski, W. Miklaszewski, A. Zeilinger, *Phys. Rev. Lett.* **85**, 4418 (2000)
19. D. Collins, N. Gisin, N. Linden, S. Massar, S. Popescu, *Phys. Rev. Lett.* **88**, 040404 (2002)
20. E. Knill, R. Laflamme, G.J. Milburn, *Nature* **409**, 46 (2001)
21. S.D. Bartlett, H. de Guise, B.C. Sanders, *Phys. Rev. A* **65**, 052316 (2002)
22. A.B. Klimov, R. Guzmán, J.C. Retamal, C. Saavedra, *Phys. Rev. A* **67**, 62313 (2003)
23. M.F. Santos, *Phys. Rev. Lett.* **95**, 010504 (2005)
24. H. Bechmann-Pasquinucci, A. Peres, *Phys. Rev. Lett.* **85**, 3313 (2000)
25. M. Bourennane, A. Karlsson, G. Björk, *Phys. Rev. A* **64**, 012306 (2001)
26. N.J. Cerf, M. Bourennane, A. Karlsson, N. Gisin, *Phys. Rev. Lett.* **88**, 127902 (2002)
27. T. Durt, N.J. Cerf, N. Gisin, M. Żukowski, *Phys. Rev. A* **67**, 012311 (2003)
28. A. Mair, A. Vaziri, G. Weihs, A. Zeilinger, *Nature* **412**, 313 (2001)
29. A. Lamas-Linares, J.C. Howell, D. Bouwmeester, *Nature* **412**, 887 (2001)
30. J.C. Howell, A. Lamas-Linares, D. Bouwmeester, *Phys. Rev. Lett.* **88**, 030401 (2002)
31. A. Vaziri, G. Weihs, A. Zeilinger, *Phys. Rev. Lett.* **89**, 240401 (2002)
32. R.T. Thew, A. Acín, H. Zbinden, N. Gisin, *Phys. Rev. Lett.* **93**, 010503 (2004)
33. H.S. Eisenberg, G. Khoury, G. Durkin, C. Simon, D. Bouwmeester, *Phys. Rev. Lett.* **93**, 193901 (2004)
34. L. Neves, G. Lima, J.G.A. Gómez, C.H. Monken, C. Saavedra, S. Pádua, *Phys. Rev. Lett.* **94**, 100501 (2005)
35. W.K. Wootters, *Phys. Rev. Lett.* **80**, 2245 (1998)
36. P. Rungta, V. Buzek, C.M. Caves, M. Hillery, G.J. Milburn, *Phys. Rev. A* **64**, 042315 (2001)
37. F. Mintert, M. Kuś, A. Buchleitner, *Phys. Rev. Lett.* **95**, 260502 (2005)
38. F. Mintert, A.R.R. Carvalho, M. Kuś, A. Buchleitner, *Phys. Rep.* **415**, 207 (2005)
39. C. Monroe, D.M. Meekhof, B.E. King, W.M. Itano, D.J. Wineland, *Phys. Rev. Lett.* **75**, 4714 (1995)
40. R. Blatt, H. Häffner, C.F. Roos, C. Becher, F. Schmidt-Kaler, *Quant. Inf. Process.* **3**, 61 (2004)
41. J.M. Taylor, C.M. Marcus, M.D. Lukin, *Phys. Rev. Lett.* **90**, 206803 (2003)
42. T. Hayashi, T. Fujisawa, H.D. Cheong, Y.H. Jeong, Y. Hirasawa, *Phys. Rev. Lett.* **91**, 226804 (2003)
43. T. Itakura, Y. Tokura, *Phys. Rev. B* **67**, 195320 (2003)
44. M. Brune, E. Hagley, J. Dreyer, X. Maître, A. Maali, C. Wunderlich, J.M. Raimond, S. Haroche, *Phys. Rev. Lett.* **77**, 4887 (1996)
45. Q.A. Turchette, C.J. Myatt, B.E. King, C.A. Sackett, D. Kielpinski, W.M. Itano, C. Monroe, D.J. Wineland, *Phys. Rev. A* **62**, 053807 (2000)
46. R. Guzmán, J.C. Retamal, J.L. Romero, C. Saavedra, *Phys. Lett. A* **323**, 382 (2004)